

# HIGHRISE BUILDING IDENTIFICATION USING TRANSIENT TESTING

M. Meyyappa (I)  
J. I. Craig (II)  
Presenting Author: J. I. Craig

## SUMMARY

Full scale forced vibration tests carried out on a 25-story steel frame building are described. A rectilinear electrohydraulic shaker was employed to produce the transient swept-sine forcing functions used as input. Modal characteristics were extracted from the measured transfer functions and utilized to adjust an a priori analytical model by varying the structural parameters assigned to the various component stiffness matrices. A weighted least squares method is proposed for identifying the structural parameters. For comparison, Bayesian estimation is also used to evaluate these parameters.

## INTRODUCTION

An often neglected component in structural design and analysis of multi-story buildings is the exterior cladding or curtain wall. The cladding, along with other architectural elements such as the interior partitions, is assumed to behave independently of the primary structure. Its mass is considered, but its stiffness is ignored and any interaction with the primary structure is minimized by designing suitable isolating connection systems. Significant interaction between the primary structure and cladding, unanticipated during design, could alter the structural behavior considerably (Ref. 1). As a part of a study aimed at cladding-structure interaction effects in highrise buildings, particularly with respect to their dynamic behavior, a 25-story steel-frame, precast concrete-clad building was analyzed using system identification techniques. Transient testing methods utilizing a special electrohydraulic exciter were employed to determine the dynamic characteristics of the building. The data were then used to improve an a priori finite element model by varying the structural parameters associated with the different components of the building, including cladding.

## TRANSIENT TESTING

Until recently, dynamic testing of highrise buildings has been almost exclusively of the steady-state or harmonic type. Transient techniques, which impart energy to the structure over the entire frequency range of interest in a short interval of time, have rarely been used. This can be traced largely to the unavailability of an exciter that fills the needs for full scale transient testing of structures like highrise buildings. Shakers must, in order to find application in building vibration tests, provide the necessary force levels as well as be capable of operating in the low frequency range which includes the natural frequencies of interest. An electrohydraulic exciter has recently been developed to meet these requirements. A brief description of this shaker is

- 
- (I) Post-doctoral research fellow  
Georgia Institute of Technology, Georgia, USA
  - (II) Professor of Aerospace Engineering  
Georgia Institute of Technology, Georgia, USA

given here; more detailed accounts can be found elsewhere (Ref. 2).

### Electrohydraulic Exciter

A schematic diagram of the exciter under discussion is shown in Fig. 1. It consists of a seismic mass that moves in a rectilinear fashion under the action of a servocontrolled hydraulic actuator. The seismic mass is made up of a set of lead weights or 'bricks' placed on a weight table whose reciprocal motion is controlled by the actuator. Four air bearings support the weight table over a smooth base plate. The arrangement is such that the reorientation of the direction of table motion is achieved by simply rotating the weight table and attached actuator on its clamping ring.

The force generated by the exciter is the inertial reaction force caused by the motion of the seismic mass. Thus it is proportional to the amplitude or stroke of the actuator and the square of the frequency. One of the distinguishing features of the exciter is its ability to produce nonsinusoidal motion of the weight table when a signal of suitable waveform is input to the servocontroller. The performance curve defining the operating range of the shaker is shown in Fig. 2. In the low frequency region (less than 1 Hz), the force produced is limited by the maximum actuator stroke, while in the intermediate range (between 1 and 3.5 Hz), the hydraulic flow rate is the constraining factor. For operating frequencies higher than 3.5 Hz, limitations arise due to the maximum allowable hydraulic pressure and the actuator piston area.

### Forcing Function

All input functions employed to drive the shaker in the full scale tests were linearly swept transient sine waveforms described by the following equation for the motion of the seismic mass:

$$x(t) = A \sin \left[ \pi (f_b - f_a) t^2 / T + 2 \pi f_a t \right] \quad (1)$$

where  $x(t)$  = swept-sine actuator motion     $f_b$  = upper frequency limit  
          $f_a$  = lower frequency limit             $T$  = sweep time  
    $A$  = amplitude

This waveform possesses a linear spectrum whose magnitude remains approximately constant between the lower and the upper frequency limits (Ref. 3). The controlling waveform is generated in a portable desktop computer by calculation at discrete time intervals and the analog signal is produced by means of a clocked digital-to-analog converter. The objective is to provide a controlled force output from the shaker, and therefore the calculated actuator stroke waveform (Eq. 1) must be suitably filtered to yield a constant force waveform. In addition, the waveform amplitude is further adjusted in order to keep the stroke, velocity and acceleration levels within physically controllable limits shown in Fig. 2 (Ref. 4).

### Vibration Testing

The building used in the present study consists of a central steel core surrounded by a lightweight exterior steel frame that supports a highly contoured precast concrete panel curtain wall. The building core is constructed with braced framing in one direction and rigid framing in the other (Fig. 3). The shaker and the peripheral equipment needed for its operation including a high pressure hydraulic pump, an air compressor and the input control system that generates the swept-sine functions were mounted on the 15th floor. The shaker itself was located at the midpoint of the north edge of the building in order to

allow excitation of both bending (two directions) and torsional response. A more desirable roof top location was not available due to power and structural limits.

Five force balance accelerometers were used to measure the dynamic response. Since the mode shape characterizations obtained from only five output measurements are usually not sufficient, the tests were carried out in two or more stages. First, the accelerometers were placed on the roof and four lower floors and a set of measurements was made. The accelerometers on the lower floors were next moved to four other floors and the tests were repeated. The roof response thus served as a reference between the two sets of measurements. Altogether, bending response measurements were made on the roof, 23rd, 21st, 19th, 17th, 15th, 12th, 9th, and 6th floors and torsional response was measured on the roof, 15th, and 10th floors. Locations and orientations for the accelerometers were chosen depending upon the type of response desired (Fig. 4).

Different frequency sweep ranges were employed to excite the building in its first few modes of interest. Lower frequency sweeps between 0.05 and 0.85 Hz, with a sweep time of 102.4 seconds, were used to measure response in the first bending and torsional modes. Sweeps between 0.1 and 4.9 Hz, with 51.2 seconds sweep time, were used for the higher modes. Separate sweeps for fundamental mode response were necessitated by the low input force levels generated by the shaker in the low frequency range. In order to initiate significant structural response in this range, it is therefore essential to traverse this region slowly so that input levels can be sustained around the resonance frequencies for sufficiently long periods of time. A portable time series analyzer, synchronized to the shaker, was used during the tests to verify proper setup and data integrity. All measurements were recorded on magnetic tape to enable extensive post-test processing of data.

## Results

Typical transfer functions calculated from the full scale forced vibration test data are shown in Fig. 5. The modal parameters were estimated by a multi-degree-of-freedom curve fitting procedure that yields complex frequencies and mode shapes (Ref. 5). Natural frequencies and damping ratios derived from the complex frequencies are listed in Table 1 for the first four modes. Real normal mode shapes obtained from the complex modes by retaining only their real parts are plotted in Fig. 6. Torsional mode shapes were handled similarly but typical results are not shown since torsional response measurements were available from only three floors.

## SYSTEM IDENTIFICATION

An a priori finite element model of the highrise building, developed for use in analytical studies of cladding effects, is described in Ref. 1. This model is made up of a lumped mass matrix and a stiffness matrix assembled from independently developed stiffness matrices for the three components, namely the primary core, the exterior frame and the cladding. An interstory shear stiffness parameter was used to quantify the stiffness effects of cladding and its connection elements on each face between floors, and the cladding stiffness matrix was developed in terms of this parameter. Preliminary ambient test results and a least squares trial and error procedure were employed to ascertain a baseline value for this parameter, which was found to be 625 Kips/inch.

In improving the a priori model with the aid of forced vibration test results, it is assumed, owing to the negligible coupling effects, that the structural response in the braced frame, rigid frame and torsional directions are

independent of each other. Each component stiffness is divided into three stiffness matrices corresponding to the three directions and a structural parameter is assigned to each of these matrices (Ref. 6). The analytical model used in identification can thus be represented by the equations of motion

$$[M]_i \{\ddot{x}\}_i + [K]_i \{x\}_i = 0 \quad (2)$$

where

$$\begin{aligned} [M]_i &= \text{mass matrix in the } i\text{th direction} \\ [K]_i &= \text{sum of component stiffnesses in the } i\text{th direction} \\ \{x\}_i &= \text{response in the } i\text{th direction} \end{aligned}$$

and a dot denotes differentiation with respect to time. The stiffness matrix can be expressed in terms of the structural parameters as

$$[K]_i = \sum_{j=1}^3 \Theta_{ij} [K]_{ij} \quad (3)$$

in which  $[K]_{ij}$  = stiffness matrix of the  $j$ th component in the  $i$ th direction  
 $\Theta_{ij}$  = structural parameter associated with  $[K]_{ij}$

When all the structural parameters are unity, one obtains the a priori model.

Allowing these parameters to assume values other than unity results in an identification method by which the analytical model defined by Eqs. (2) and (3) can be made to reproduce experimentally measured modal parameters as accurately as possible. When the stiffness is modelled as in Eq. (3), however, the procedure is not as effective in improving the analytical mode shapes without producing excessive changes in the a priori values of the structural parameters. This is especially true if the initial mode shapes differ substantially from the experimental data as will be seen later.

A priori model frequencies are listed with experimental frequencies in Table 1, while the a priori mode shapes are compared to the measured modes in Fig. 6. Also given in Table 1 are the values of the sum of squares of errors (SSQ), which is one measure of the closeness of the analytical values to the test results.

Evaluation of the nine structural parameters, three in each direction corresponding to the three components, is carried out using two methods: the standard Bayesian technique and a weighted least squares approach. Both procedures take into account the uncertainties in the experimental results as well as those in the analytical model. It is assumed that the measurement and modelling errors can be represented by specifying an error covariance matrix for the measurements and prior mean and covariance matrices for the parameters to be estimated.

#### Bayesian Estimation

If the measurement errors and the prior density function are taken to be normally distributed, Bayesian estimation is equivalent to minimizing the cost or objective function (Ref. 7)

$$\Psi = \{e\}^T [V_y]^{-1} \{e\} + \{\Theta - \mu\}^T [V_\Theta]^{-1} \{\Theta - \mu\} \quad (4)$$

where  $\{e\}$  =  $\{Y\} - \{F\}$ , the error vector  
 $[V_y]$  = measurement error covariance matrix  
 $\{\Theta\}$  = structural parameter vector  
 $\{\mu\}$  = prior mean of the structural parameters

- $[V_{\Theta}]$  = prior covariance of the structural parameters  
 $Y_i$  = ith measured value, either a frequency or a mode shape coefficient  
 $F_i$  = ith analytical value corresponding to  $Y_i$

#### Weighted Least Squares Estimation

The cost function for this case is defined by

$$\Psi = \{e\}^T [W] \{e\} \quad (5)$$

with the weighting matrix  $[W]$  taken as

$$[W] = [V_e]^{-1} \quad (6)$$

where  $[V_e]$  is the error covariance obtained by treating both  $\{Y\}$  and  $\{F\}$  as random. If the experimental and analytical values are uncorrelated, it follows that

$$[V_e] = [V_y] + [V_F] \quad (7)$$

where  $[V_F]$  is the covariance matrix of the analytical values, which can be shown to be (Ref. 8)

$$[V_F] = \left[ \frac{\partial F}{\partial \Theta} \right]^T [V_{\Theta}] \left[ -\frac{\partial F}{\partial \Theta} \right] \quad (8)$$

in which

$$\left( \frac{\partial F}{\partial \Theta} \right)_{ij} = \frac{\partial F_j}{\partial \Theta_i}, \text{ evaluated at } \{\Theta\} = \{\mu\}$$

It should be noted that in the above procedure no assumptions are made concerning the distribution of the measurement errors or the prior density function other than requiring that the mean and covariance matrices be known.

#### Results

Minimization of the objective functions defined by Eqs. (4) and (5) was accomplished by using the inverse rank one correction (IROC) method (Ref. 7). Derivatives of the analytical frequencies and mode shapes, required to compute  $[V_F]$  and also to evaluate the gradient of the objective function during each iteration, were determined using well established procedures (Ref. 8). Diagonal covariance matrices  $[V_y]$  and  $[V_{\Theta}]$  were calculated with assumed values of standard deviations for the measurements and the structural parameters. For all the measured frequencies, 0.2% standard deviation was assumed. On the other hand, values of 5, 10, and 15% standard deviation were used for the first, second and third mode shapes respectively. This is due to the fact that mode shape measurements are usually much less accurate than the frequencies and the uncertainty involved in mode shape estimation from transfer functions is more for higher modes. Prior mean values for all the structural parameters were set equal to one and prior covariance was found using 3, 4 and 5% standard deviations for the core, frame and cladding parameters, respectively. In the weighted least squares approach, all off-diagonal terms in  $[V_e]$  were ignored when computing  $[W]$  (Ref. 4). With this simplification, the procedure is equivalent to assigning weights to various error terms based on the variance of the experimental and the analytical modal parameters.

The structural parameter values arrived at by identification are listed in Table 2 for various cases. Both estimation procedures yield approximately the same results in all three directions. When mode shapes are also included, the

values are again close in the braced frame direction. But in the rigid frame direction where a priori mode shapes are quite different from test data (Fig. 6), weighted least squares estimates undergo large changes from the initial value of unity, though a substantial reduction in the SSQ (82%) is obtained. This does not occur in the Bayesian procedure since, in this case, the parameters are constrained by the prior density term in the cost function in Eq. (4). Consequently, the procedure fails to decrease the error significantly, giving a reduction of only 4% in the SSQ. A study of Table 2 reveals that the cladding parameter is highest in torsion, which implies that the effect of cladding is more in torsion than in bending, in agreement with the findings reported in Ref. 1. It is also seen that the weighted least squares method consistently produces estimates with lower error.

#### CONCLUSIONS

Application of an electrohydraulic exciter, designed to generate transient forcing inputs, in full scale tests has been demonstrated. A swept-sine testing technique has successfully been implemented using this shaker. Such testing procedures require far less time and effort when compared to the conventional harmonic testing method. A weighted least squares estimation scheme has been described for use in system identification and has been found to perform satisfactorily in evaluating the structural parameters associated with the building components.

#### REFERENCES

1. Goodno, B. J., and Palsson, H., "Torsional Response of Partially-Clad Structures," Proceedings, Conference on Earthquakes and Earthquake Engineering, held at Knoxville, Tennessee, Sept. 1981, pp. 859-877.
2. Craig, J. I., and Lewis, F. D., "A Rectilinear Force Generator for Full Scale Vibration Testing," Proceedings, 2nd ASCE/EMD Specialty Conference on Dynamic Response of Structures, held at Atlanta, Georgia, Jan. 1981, pp. 102-110.
3. White, R. G., and Pinnington, R. J., "Practical Application of the Rapid Frequency Sweep Technique for Structural Frequency Response Measurement," The Aeronautical Journal, Vol. 86, No. 855, May 1982, pp. 179-199.
4. Meyyappa, M., "Identification of Cladding-Structure Interaction in Highrise Buildings Using Parameter Estimation Methods," Ph.D. Dissertation, School of Aerospace Engineering, Georgia Institute of Technology, Atlanta, Georgia, Mar. 1982.
5. Richardson, M., and Potter, R. W., "Identification of the Modal Properties of an Elastic Structure from Measured Transfer Function Data," Proceedings, 20th ISA Symposium, held at Albuquerque, New Mexico, May 1974, pp. 239-246.
6. Torkamani, M. A. M., and Hart, G. C., "Earthquake Engineering: Parameter Identification," Preprint No. 2499, ASCE National Structural Engineering Convention, held at New Orleans, Louisiana, April 1975.
7. Bard, Y., Nonlinear Parameter Estimation, Academic Press, New York, 1974.
8. Collins, J. D., and Thomson, W. T., "The Eigenvalue Problem for Structural Systems with Statistical Properties," AIAA Journal, Vol. 7, No. 8, April 1969, pp. 642-648.

TABLE 1. Modal Data

		BRACED FRAME DIRECTION			RIGID FRAME DIRECTION			TORSION			
		EXPERIMENTAL		A PRIORI	EXPERIMENTAL		A PRIORI	EXPERIMENTAL		A PRIORI	
MODAL PARAMETERS	MODE NO.	Freq. (Hz)	Damp. (%)	Freq. (Hz)	Freq. (Hz)	Damp. (%)	Freq. (Hz)	Freq. (Hz)	Damp. (%)	Freq. (Hz)	
		1	0.41	2.7	0.402	0.32	4.2	0.345	0.41	4.3	0.408
		2	1.30	1.4	1.263	0.96	2.4	0.995	1.23	3.5	1.174
		3	2.35	3.0	2.349	1.68	3.3	1.778	2.09	5.5	2.000
		4	3.37	2.3	3.273	2.32	4.7	2.366	2.92	4.9	2.776
SSQ	4 Freq.	0.108 x 10 <sup>-1</sup>			0.179 x 10 <sup>-1</sup>			0.322 x 10 <sup>-1</sup>			
	4 Freq. + 3 Mode Shapes	0.197			0.590			—			

TABLE 2. Structural Parameter Estimates

METHOD	DIRECTION	4 FREQUENCIES ONLY				4 FREQUENCIES + 3 MODE SHAPES			
		CORE	FRAME	CLADDING	SSQ	CORE	FRAME	CLADDING	SSQ
BAYESIAN	BRACED FRAME	1.043	0.949	1.023	$.334 \times 10^{-2}$	1.043	0.948	1.024	.189
	RIGID FRAME	0.895	0.938	0.903	$.662 \times 10^{-2}$	0.894	0.939	0.905	.569
	TORSION	1.049	1.015	1.081	$.418 \times 10^{-2}$	—	—	—	—
WEIGHTED LEAST SQUARES	BRACED FRAME	1.043	0.963	1.023	$.332 \times 10^{-2}$	1.043	0.940	1.059	.189
	RIGID FRAME	0.904	0.952	0.916	$.537 \times 10^{-2}$	0.323	0.890	1.850	.106
	TORSION	1.051	1.023	1.081	$.395 \times 10^{-2}$	—	—	—	—

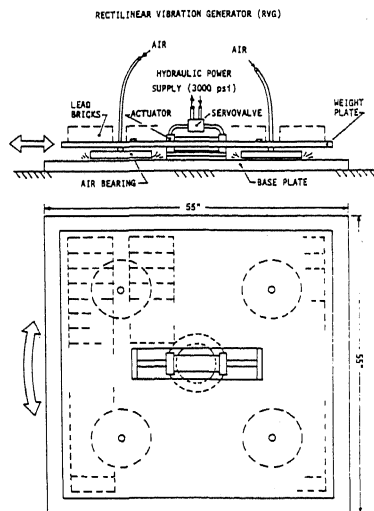


Figure 1. Shaker Schematic

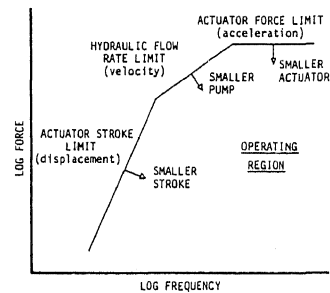


Figure 2. Performance Curve

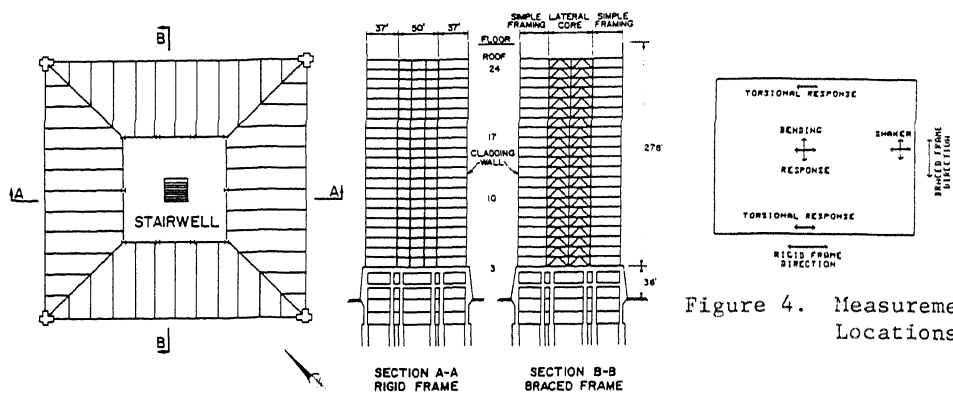


Figure 3. Structural Framing

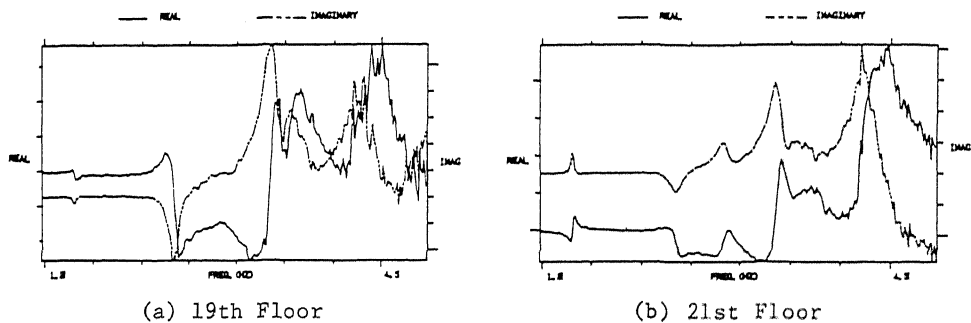


Figure 5. Transfer Functions in Braced Frame Direction

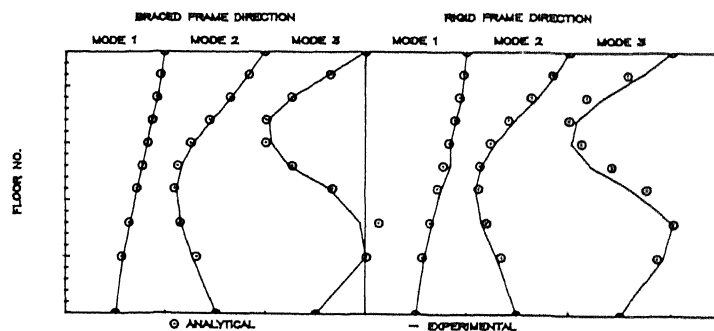


Figure 6. Mode Shapes